



Displacement Reactions Between Metal Ions and Nitride Barrier Layer/Silicon Substrate

Y. Wu,* W. C. Chen, H. P. Fong, C. C. Wan,** and Y. Y. Wang^z

Department of Chemical Engineering, National Hsing-Hua University, Hsinchu, Taiwan

Nitride materials such as TiN and TaN have been used in the integrated circuit industry. These materials serve as the crucial barrier layer between copper and the dielectric layer, and hence should be chemically inert. However, a displacement reaction still occurs between these nitride barriers and some metal ions such as Cu^{2+} , Ag^+ , and Pd^{2+} in the presence of F^- . This spontaneous reaction results in the deposition of metal, and a similar reaction takes place between the metal ions and the underlying silicon substrate. Three possible mechanisms are proposed and discussed in this study. The proposed mechanisms and the details of displacement reaction were elucidated by using Auger electron spectroscopy, X-ray photoelectron spectroscopy, scanning electron microscopy, nuclear magnetic resonance spectroscopy, inductively coupled plasma atomic emission spectrometer, Raman and infrared spectroscopy. TiN was found to oxidize with the formation of TiF_6^{2-} . Despite being regarded as a contaminant, the deposited Pd was found to be capable of serving as the platform on nitride barrier for subsequent electrodeposition of Cu.

© 2002 The Electrochemical Society. [DOI: 10.1149/1.1464885] All rights reserved.

Manuscript received July 16, 2001. Available electronically March 29, 2002.

To improve function and efficiency, the feature size of a chip has been shrunk to the submicrometer level. Therefore the interconnections between devices and gates have become very important.¹⁻⁴ Cu is regarded as the best material for these interconnections because it possesses low resistivity, high melting point, and superior electromigration endurance.⁵ The conventional method is to form a Cu interconnection from the electrodeposition of Cu. This process is executed on a Cu seed layer previously deposited by the chemical vapor deposition (CVD) or physical vapor deposition (PVD) process. This seed layer is capable of conducting electricity for electrodeposition. Electroless copper has also been studied but is still in the development stage.

Nitride barrier materials,⁶⁻⁹ such as TiN and TaN, have been developed to solve the problem of Cu thermal diffusion into dielectric SiO_2 . TiN is a typical polycrystalline material with a small grain size of about 10-50 nm. TiN has been used to serve as a barrier material because of its high rigidity, high melting point (2930°C), good thermal and electrical conductivity, high thermal stability, and good manufacturing properties. A single-phased TiN possesses a face-centered cubic (fcc) structure similar to that of NaCl, and its lattice constant is equal to 4.24 Å. The properties of TaN approach those of TiN, *i.e.*, possessing high rigidity, high melting point (3090°C), high thermal stability, and inert chemical properties. The crystal structure of TaN is also with a single-phased lattice constant equal to 4.33 Å. However, the electrical resistivity of TaN is higher than that of TiN. At room temperature TaN has an electric resistivity of 135-170 $\mu\Omega$ cm, whereas that of TiN is 100-150 $\mu\Omega$ cm. Both can be deposited by the chemical vapor deposition (CVD) or plasma vapor deposition (PVD) process.

The main function of the diffusion barrier is to prevent Cu atoms from penetrating into the dielectric layer. It also improves the adhesion of the conducting layer. Therefore, barrier materials must have superior chemical stability. However, the displacement reaction between the nitride barrier layer/Si substrate and metal ions has been reported. Dubin *et al.*¹⁰ reported that Cu deposition occurs as a result of the displacement reaction of TiN/Si. Fung *et al.*¹¹ also reported such deposition due to the displacement reaction between Cu^{2+} and the underlying Si with cracks in the intermediate TiN film. O'Kelly¹² proposed that a Cu layer could be obtained by electroless plating following pretreatment with Pd which had been presumably deposited via a displacement reaction. Although metal deposition has been reported, few of the studies have explained the reactions involved. This study aims to elucidate further the mechanisms of the

displacement reaction. A better understanding of the chemical properties of nitride barriers will help in assessing their feasibility. Moreover, the metal deposits from a displacement reaction could serve as a seed layer for subsequent electroless Cu deposition instead of being regarded as contaminants. Therefore, we applied Cu electrodeposition directly onto the nitride barrier following the displacement deposition of metal seed.

Experimental

From previous studies, we believed that metal ions other than Cu^{2+} could deposit on the barrier layer through a displacement reaction under suitable conditions. Three different metallic ions were chosen and prepared as activation solutions. The composition of the solution was metal ion 0.01 M and $\text{NH}_4\text{F}\cdot\text{HF}$ (BHF) 0.1 M. Si wafers were cut into 1 cm^2 samples ready for deposition testing. The edges of the samples were sealed with wax to prevent interaction between exposed Si/ SiO_2 and metal ions. Wafer samples were then examined by Auger electron spectroscopy (AES), X-ray photoelectron spectroscopy (XPS), scanning electron microscopy (SEM), nuclear magnetic resonance spectroscopy (NMR), inductively coupled plasma in an atomic emission spectrometer (ICP-AES), Raman and infrared (IR) spectroscopy to elucidate the mechanism of these reactions and the morphology of the deposits. Cu was deposited on the surface following the displacement reaction in order to assess its industrial feasibility. The process flow is schematized in Fig. 1. In this case, TaN and Pd were chosen as the barrier material and the metallic seed, respectively. The deposition bath was a typical acidic bath, containing $\text{CuSO}_4\cdot 5\text{H}_2\text{O}$ 70 g/L, H_2SO_4 10 mL/L. The barrier-layer materials used were 50 nm thick TiN and TaN, which were deposited by sputtering. n-Type (111) single-crystal Si samples were used as the underlying substrate.

Results and Discussion

Three different kinds of metallic ions were chosen to test their ability to initiate a displacement reaction in the presence of BHF. All selective ions possess a relatively high reduction potential. Table I shows the results of different solutions in contact with various substrates. It is worth noting that metal deposition by displacement reaction happens only in the presence of F^- . F^- tends to corrode the barrier layer under acidic conditions. However, how F^- induces a displacement reaction with the barrier layer remains unknown. According to Table I, TiN film can react with Cu^{2+} , Ag^+ , and Pd^{2+} . However, TiN powder was found less reactive than TiN film. It only reacted with Ag^+ and Pd^{2+} . Two reasons were proposed to explain this difference. The first is that F^- may corrode and crack the surface of the TiN film. The electrolyte then penetrates and initiates a displacement reaction between the underlying Si and metal ions.

* Electrochemical Society Student Member.

** Electrochemical Society Active Member.

^z E-mail: yywang@mx.nthu.edu.tw

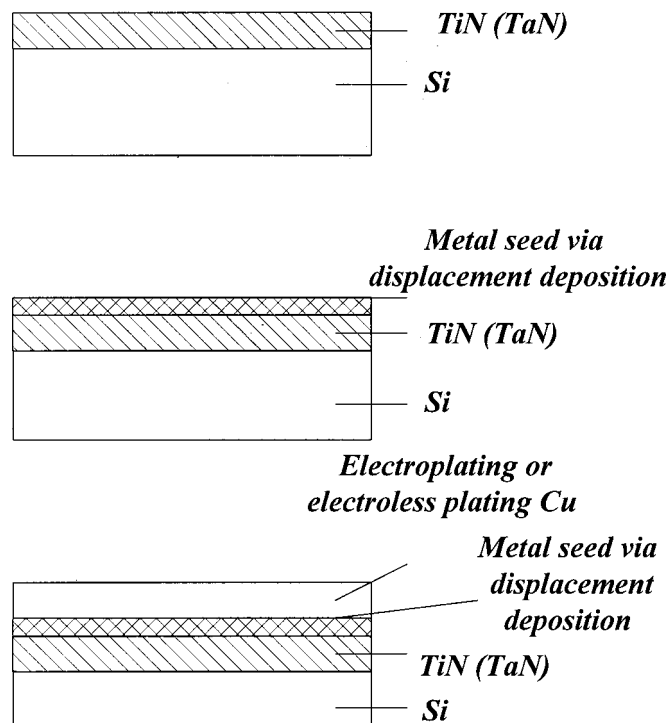


Figure 1. Process flow of Cu metallization via displacement deposition.

The second is that the grain size of TiN powder is much larger than that of the sputtered TiN film. This could strongly influence the activity of these two materials. The metal deposition observed may have resulted from the contact between Si and the solution if the metal ions have indeed penetrated the TiN surface. However, SEM detected no significant corrosion of TiN film, therefore the second explanation is more plausible. It was also found that TaN film could only be displaced by Pd^{2+} which has the most positive reduction potential of all the selected metal ions. This finding indicates that TaN is even more chemically inert than TiN.

Also noteworthy is that this reaction occurs solely under pH conditions between 3.5 and 5. In a more acidic environment, the corrosion by F^- would overwhelm the displacement reaction. F^- would penetrate the barrier film, inducing side reactions between the underlying SiO_2/Si and metallic ions. Under alkaline conditions, the displacement reaction would not even take place.

Unlike Cu or Ag deposition, Pd deposition cannot be detected visually. SEM was employed to identify the existence of metal deposits, as shown in Fig. 2. The grain size of Pd is in the range from 0.1 to 0.5 μm , which is the smallest among all deposits. In addition, all the metal deposits tended to reside island-wise rather than in a continuous film. It is known from Table I that metal deposition on either the TiN, TaN, or Si substrate cannot take place without the presence of F^- plays an essential role in the reaction. However, the interference from the possible reaction between underlying Si and metal ions must be eliminated. Therefore, AES was used to analyze the interface of miscellaneous films on the substrate. Figure 3 illustrates the AES depth profile of the substrate after being immersed in a Pd displacement solution. It is observed that Pd did not penetrate through the TiN barrier film. This implies that the underlying SiO_2/Si is not involved in this reaction, *i.e.*, the edge-sealing wax and the barrier film successfully retarded the penetration of the BHF solution. Therefore, we can conclude that displacement reaction indeed occurred between TiN and metal ions.

According to the above description, this reaction should involve a cumbersome procedure instead of a simple redox reaction like the M^{z+} -Ti couple. It is known that NH_3 or other compounds containing the N-H group are needed in the formation of TiN and that a stabi-

Table I. Displacement reaction between metal ions and barrier materials.

Solution	Si	TiN film	TiN powder	TaN film	Ti
$\text{F}^-/\text{Cu}^{2+}$	○	○	X	X	○
F^-/Ag^+	○	○	○	X	○
$\text{F}^-/\text{Pd}^{2+}$	○	○	○	○	○
BHF	●	X		X	●
Cu^{2+} (0.337 V)	X	X	X	X	○
Ag^+ (0.799 V)	X	X	X	X	○
Pd^{2+} (0.987 V)	X	X	X	X	○

Time: 15 min. Temp: 20°C.

Symbol ○ represents that the deposition of metal was observed.

Symbol X represents that no reaction was observed.

Symbol ● represents that the corrosion of substrate was observed.

lization procedure is required for the entire process.⁷ The N-H functional group could remain on the surface due to incomplete stabilization. The residual N-H functional group, being an effective reducing agent, may induce the redox reaction. Accordingly, the first conceivable mechanism is the metal deposition due to the catalysis of surface hydrogen atoms. Figure 4 is a scheme of this mechanism. If the reaction does follow this path, the N-H functional group on the TiN surface should be examined. Therefore, XPS was applied to analyze the surface of the TiN-coated Si wafer. However, no N-H functional group existed on the TiN surface. It is also known that some titanium compounds possess a catalytic ability to promote photocatalytic or photolysis reaction. Therefore, the second possible mechanism is the reduction of metal ions by photochemical reaction. According to this mechanism, metal atoms are deposited cathodically by the electrons being released through photoexcitation of TiN, as shown in Fig. 5. In investigating this mechanism, two solutions of identical composition were prepared. One was exposed under illuminated UV light, while the other was not. Since no difference was observed between the two, the second possible mechanism had no evidence to support it.

The third mechanism proposed was the deposition of metal atoms resulting from galvanic oxidation of TiN, *i.e.*, metal ions receive electrons released by the oxidation of TiN, as illustrated in Fig. 6. To verify this mechanism, it is necessary to confirm that titanium had indeed been oxidized after the ejection of electrons. The oxidation state of titanium was measured by XPS before and after the reaction, as shown in Fig. 7 and 8, respectively. In Fig. 7, the peak at 455.8 eV stands for the binding energy of the electrons at $2p_{3/2}$ orbital, while the peak at 461.6 eV represents that at $2p_{1/2}$ orbital. The two peaks illustrate that titanium was in the state of Ti-N bonding. In Fig. 8, the two peaks at 458.4 and 463.8 eV appeared after the displacement reaction with Pd^{2+} , which implies that titanium is oxidized during Pd deposition. This phenomenon also appears in the displacement with Cu^{2+} or Ag^+ . According to a previous study,¹³ it is possible that TiN is oxidized to form TiO_x or titanium halide. This corresponds to the hypothesis of the third mechanism. However, the deposition of metal by a displacement reaction only took place in the presence of F^- . Thus, the effect of F^- must be further investigated.

A halide, like F^- , possesses the catalytic ability of a bridging ligand. This had been described by Franklin *et al.*¹⁴ Thus, F^- is capable of serving as a bridging ligand between Pd^{2+} and Ti on the substrate surface. Accordingly, the existence of the Pd^{2+} complex must be verified. However, to our knowledge, there is a lack of literature describing the combination of the Pd^{2+} complex with F^- . NMR and Raman spectroscopy were used to confirm that F^- is capable of serving as ligand in the Pd^{2+} complex. NMR showed various bonding types of F^- before and after the reaction, as shown in Fig. 9 and 10, respectively. Some identical peaks could be observed in both figures. The peak at 129.02 ppm should represent the

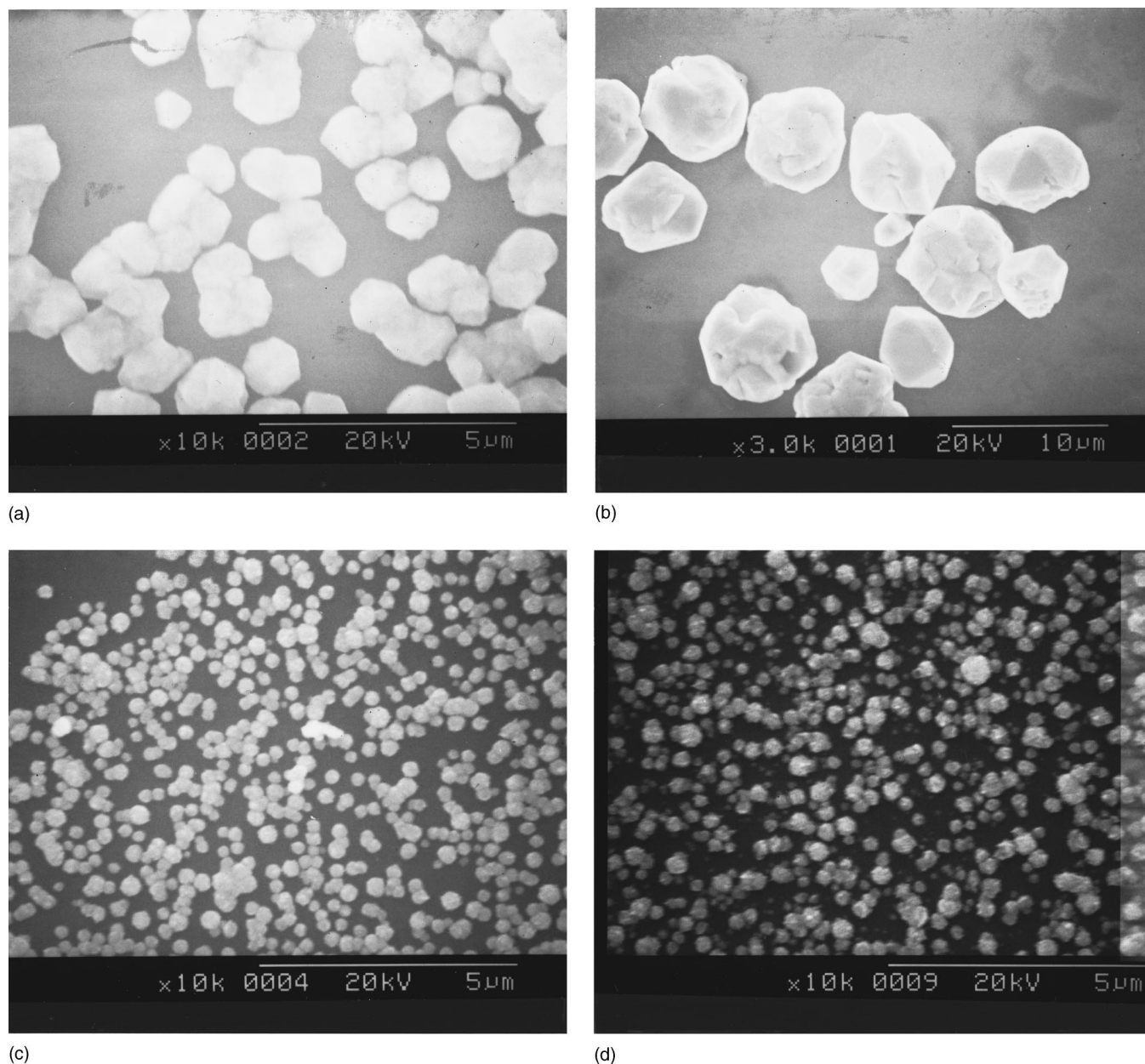


Figure 2. Metal deposit on the surface of nitride barrier by displacement reaction. (a) Cu deposits on TiN at a magnification of 10 k. (b) Ag deposits on TiN at a magnification of 3 k. (c) Pd deposits on TiN at a magnification of 10 k. (d) Pd deposits on TaN at a magnification of 10 k.

unbonded F^- , whose magnetic field is less shielded by the adjacent electron field. The decline and chemical shift of the peak from 151.76 ppm to 154.2 ppm is obvious. The declining intensity implies that the amount of F^- bonding decreases because of the displacement reaction. Accordingly, the shifted peak is assumed to be the bonding state in which F^- serves as a ligand in a square planar palladous complex. In addition, the chemical shift in this peak reveals that the original complex bonding might have been interfered with or even replaced by other generated species, *e.g.*, titanium halide. Moreover, BHF was replaced by NaF to eliminate the possible interference from ammonium. The result correlated to that of a previous experiment, as shown in Fig. 11 and 12. The shifted peak, which should stand for the ligand-fluoride, also shifted from 148.87 to 151.05 ppm. This finding therefore reveals a similar electron shielding as that of the reaction product above.

Raman spectroscopy provided additional evidence for the formation of a Pd-F complex. No scattering peaks were displayed in a

pure NaF solution. However, the peaks, 291 and 339 cm^{-1} , appeared after the addition of $PdCl_2$, as shown in Fig. 13 and 14, respectively. The frequency of the two peaks, to some degree, corresponds to the stretching and scissoring vibrational modes of $PdCl_4^{2-}$ complex, 303 and 275 cm^{-1} , respectively.¹⁵ It is claimed that the deviation of the vibrational frequency is due to the ligand replacement of Cl^- by F^- . Therefore, the resulting complex before we proceeded with the displacement reaction was assumed to be $PdCl_xF_y^{2-}$; the sum of x and y is 4 due to the limitation in the number of ligands in the square planar complex. Both of the above-mentioned peaks disappeared after the displacement reaction continued for 24 h, *i.e.*, all Pd^{2+} were almost consumed, as shown in Fig. 15. The result also implies the consumption of Pd^{2+} complex in the reaction.

Another interesting phenomenon was observed on the TiN/SiO₂/Si samples not sealed with wax. In these cases, SiO₂ was

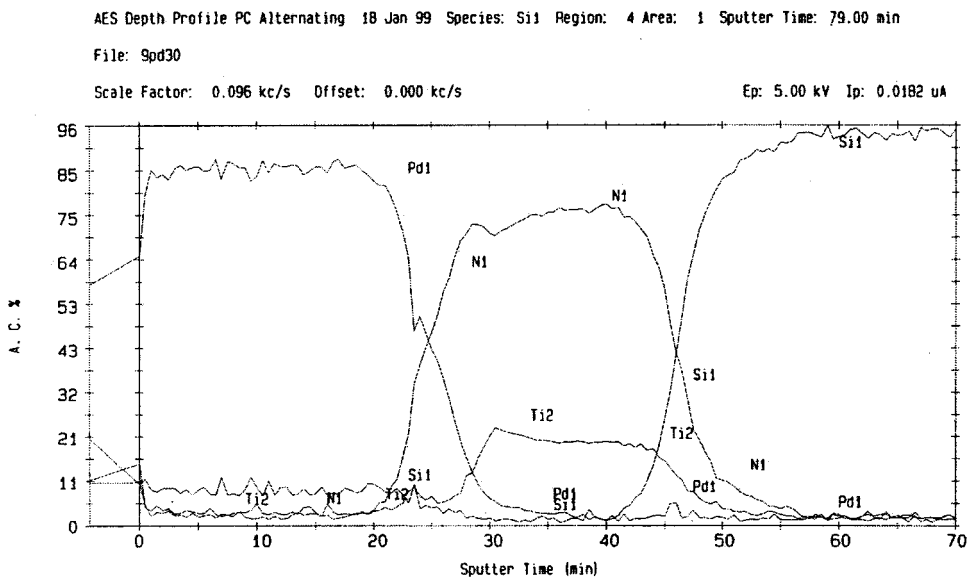


Figure 3. AES depth profile of sample after being immersed in Pd displacement solution.

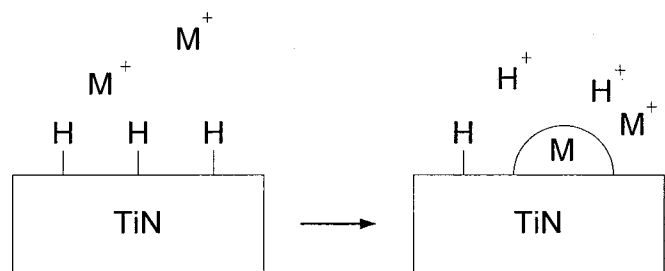


Figure 4. First possible mechanism via hydrogen-termination reaction on TiN.

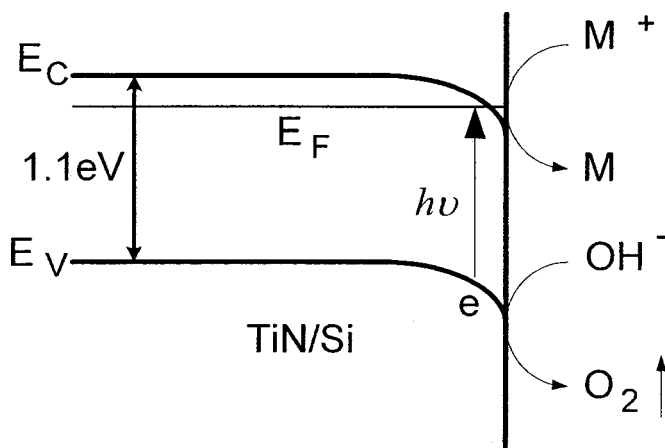


Figure 5. Second possible mechanism through photochemical reaction.

exposed to solutions containing F^- . A large amount of crystals with irregular needle shapes were formed, as shown in Fig. 16. Generally, the deposits of metal clusters were circular in shape. Hence, the crystals found on the substrate were probably inorganic salts. Interestingly, these salts could not be observed if the edges of samples were sealed with wax. The needle-shaped salt was also found on the surface when TaN was used as the barrier instead of TiN. The IR

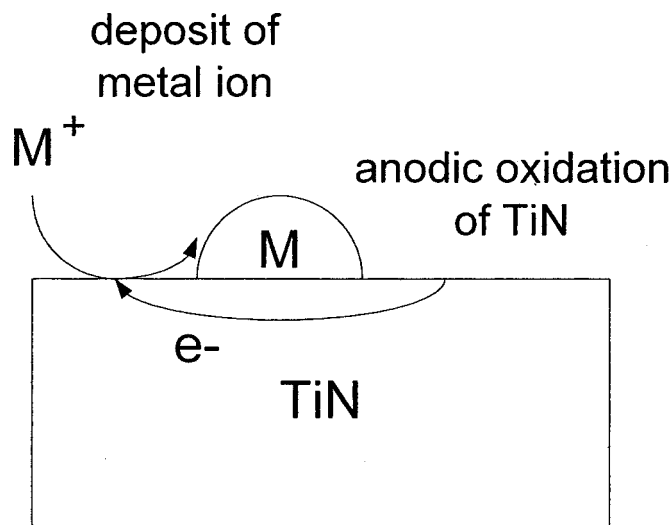


Figure 6. Anodic oxidation of TiN and cathodic reduction of metal ion in third mechanism.

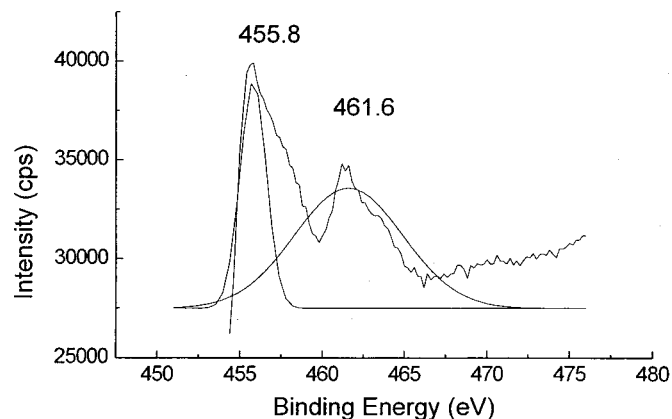


Figure 7. Oxidation-state of Ti before displacement reaction.

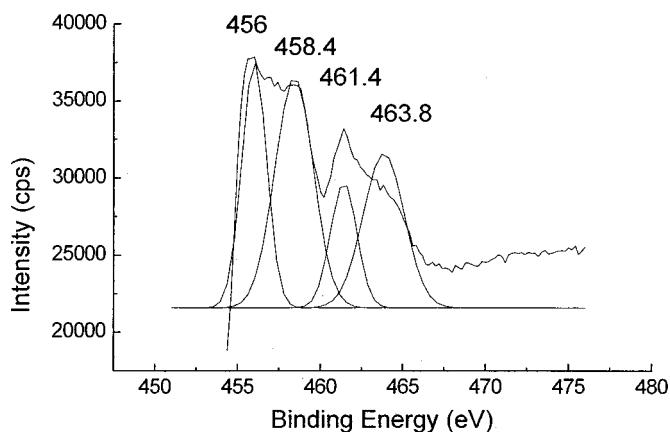


Figure 8. Oxidation-state of Ti after displacement reaction with Pd^{2+} .

spectra before and after Cu displacement on the unsealed nitride samples are displayed in Fig. 17 and 18, respectively. A comparison between the two spectra suggests that most of the absorption peaks are consistent. For instance, the absorption at 3130 and 1401 cm^{-1} comes from the stretching and bending vibration of the N-H functional group due to NH_4^+ . The peak at 1226 cm^{-1} represents the absorption of HF_2^- . However, two distinctive absorption peaks appeared, 481 and 738 cm^{-1} . According to previous research,¹⁵ the inorganic salts found should be $(\text{NH}_4)_2\text{SiF}_6$. Si samples without a nitride barrier were dipped into various activation solutions to illustrate the formation of $(\text{NH}_4)_2\text{SiF}_6$, and the result corresponded to that of our previous finding. Therefore, we believe that the reduction of metal ion on Si would not be initiated until the oxidation of Si took place. Consequently, we propose the following two-step reaction to describe the oxidation of Si and the corrosion of SiO_2 .

First step, corrosion of SiO_2

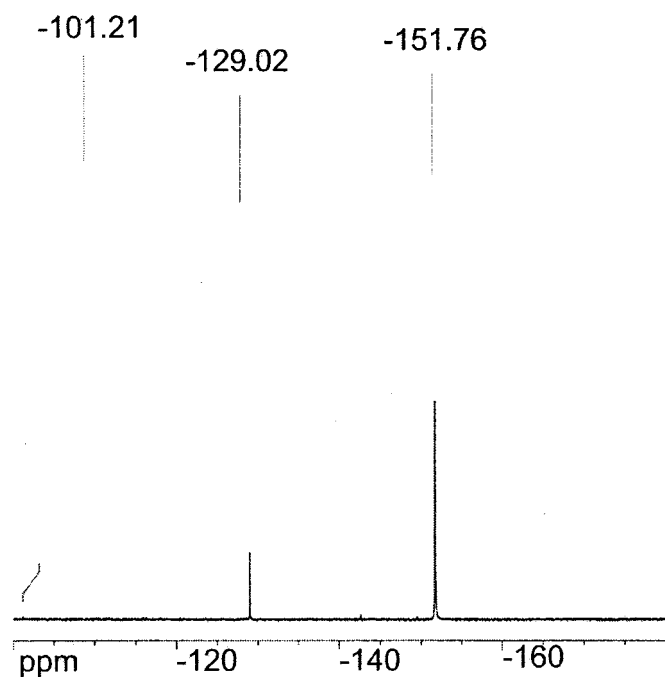


Figure 9. NMR spectra of F^- provided by BHF before the displacement reaction.

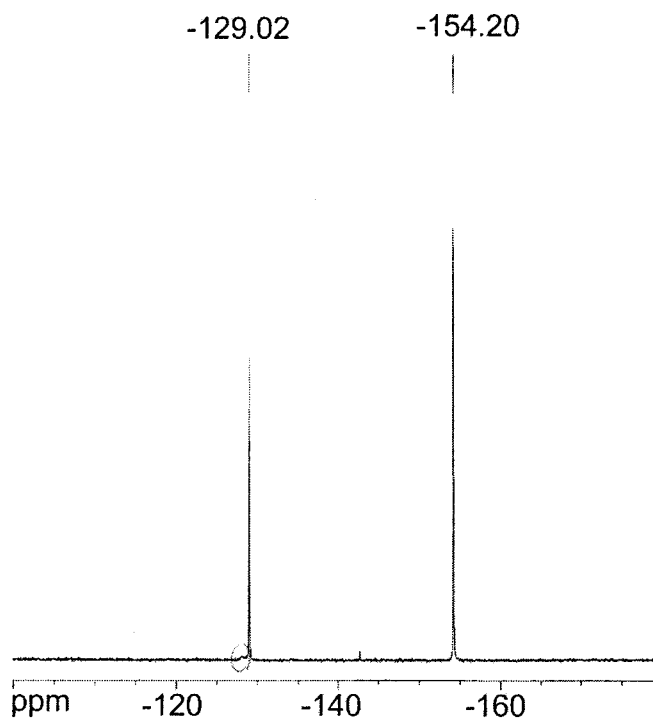
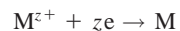


Figure 10. NMR spectra of F^- provided by BHF after the displacement reaction.

Second step, oxidation of Si



reduction of metal ion



-100.68 -129.20 -148.87

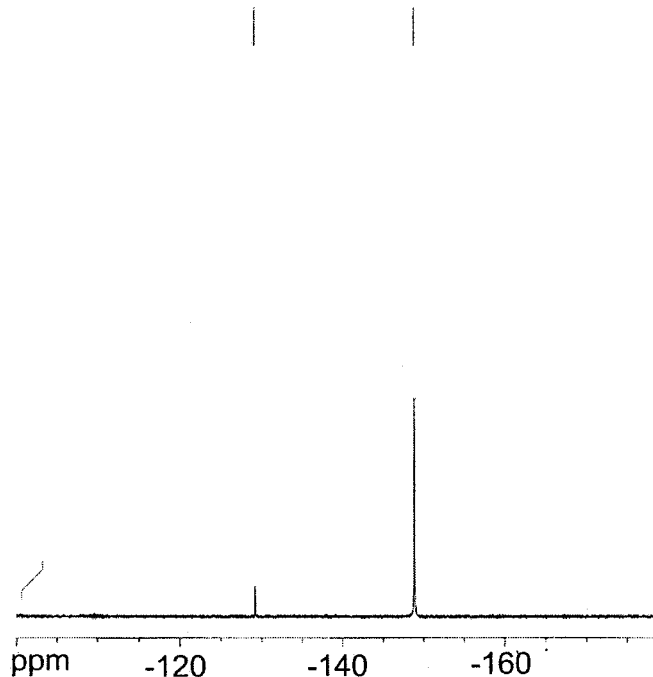


Figure 11. NMR spectra of F^- provided by NaF before the displacement reaction.

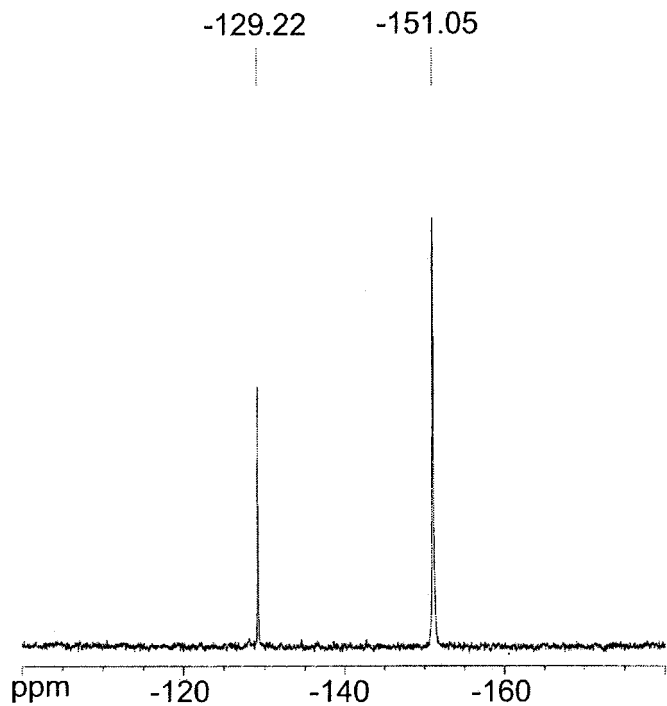


Figure 12. NMR spectra of F^- provided by NaF after the displacement reaction.

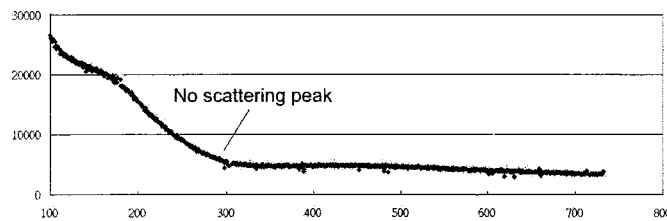


Figure 13. Raman spectra of NaF solution.

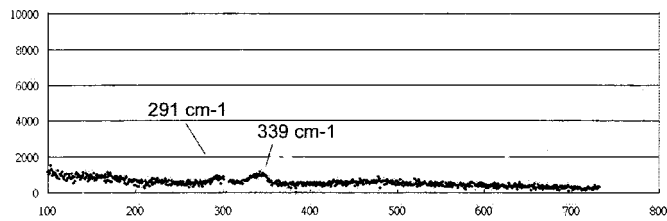


Figure 14. Raman spectra of NaF + $PdCl_2$ solution.

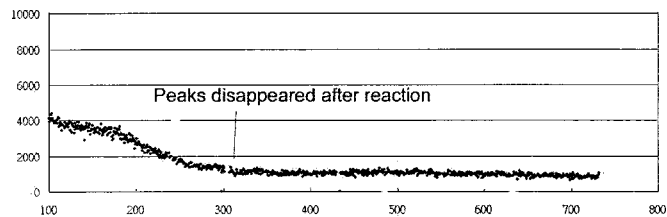


Figure 15. Raman spectra of solution after displacement reaction.

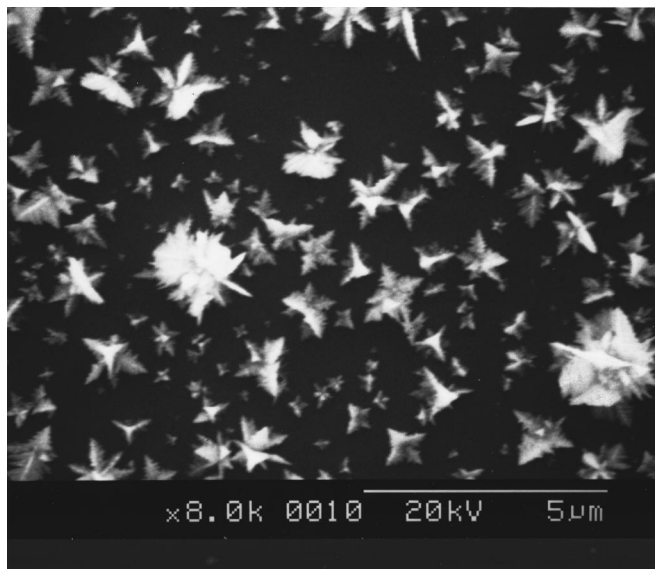


Figure 16. Needle-shape crystals found on the unsealed substrate.

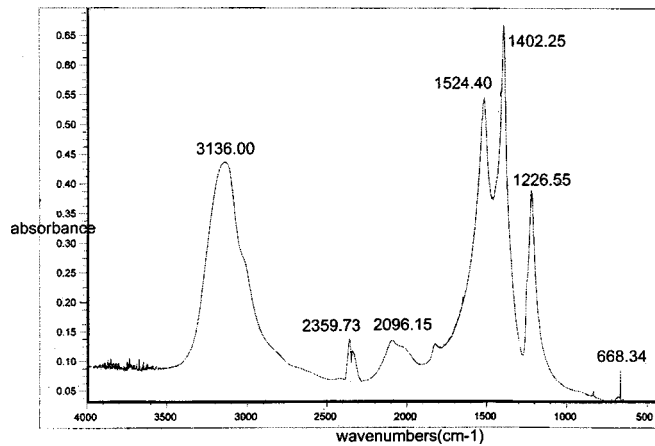


Figure 17. IR spectra before Pd displacement reaction on unsealed TaN/Si sample.

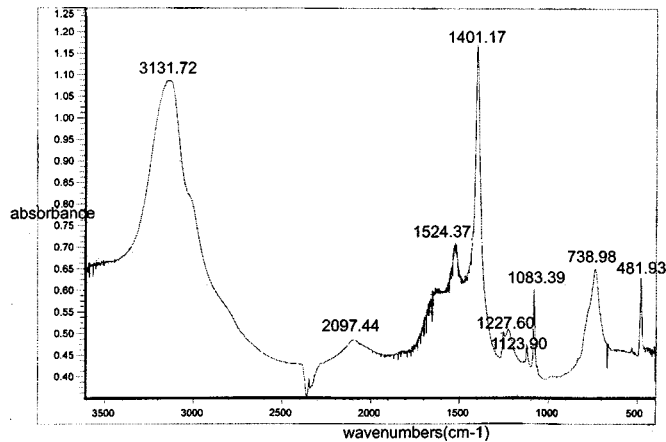


Figure 18. IR spectra after Pd displacement reaction on unsealed TaN/Si sample.

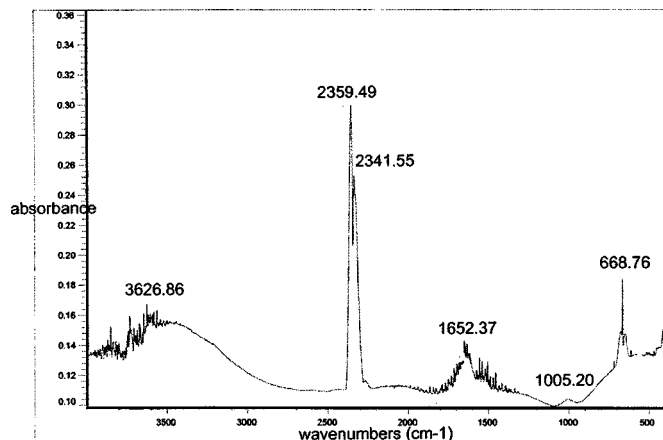
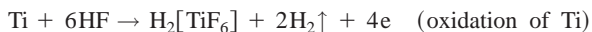


Figure 19. IR spectra of Pd activation solution before TiN reacting with Pd^{2+} .

Initially, F^- corrodes the exposed SiO_2 to form SiF_6^{2-} which precipitates slightly into $(\text{NH}_4)_2\text{SiF}_6$. Once the SiO_2 film is penetrated, the underlying Si releases electrons which are captured by metal ions. Thus, metal deposition occurs at the second step when the oxidation of Si takes place.

Kelly *et al.*¹³ once suggested a mechanism for the displacement reaction of TiN, in which TiN is oxidized to form TiF_6 together with the reduction in Pd^{2+}



However, there are two questionable points in the above mechanism. The first is that titanium cannot possibly reside in a TiN structure in an unbonded elemental state, which can be demonstrated in both Fig. 7 and 8. The structure of TiN, similar to NaCl, is much closer to ionic bonding than covalent bonding. Moreover, the nitrogen atom is usually bonded with other metallic ions in the state of nitride, N^{3-} . Hence, the state of titanium in TiN film could be regarded as Ti^{3+} . The second is that the reduction of H^+ makes the first half of the reaction charge unbalanced. Hence, the mechanism needs to be modified. Figure 19 and 20 are the IR spectra of TiN/ SiO_2 / Si samples after reacting with Pd^{2+} ions. The competitive reaction of the underlying Si had been eliminated by sealing the edges with wax. In both figures, peaks at about 2359, 2341, and 668 cm^{-1} all resulted from the interaction between the solvated TiN and

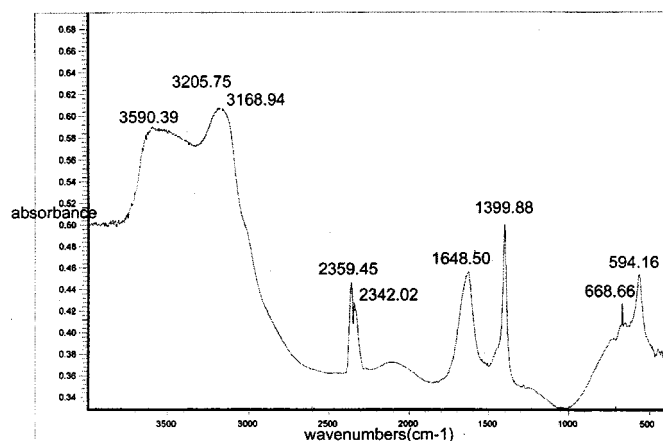


Figure 20. IR spectra of Pd activation solution after TiN reacting with Pd^{2+} .

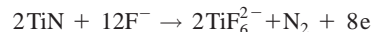
Table II. ICP result for displacement reaction between TiN and Pd^{2+} .

Sample description	Component weight (μg)	Relative concentration (ppm)
A. BHF + PdCl_2 (Before reaction)	Pd 18.787 Ti 0.0	375.74 0
B. BHF + PdCl_2 + TiN (After reaction)	Pd 0.351 Ti 33.900	7.02 678
C. BHF + TiN	Ti 0.528	5.28

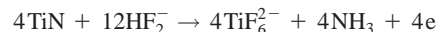
solvent or vibrations of the solvated Ti-N bonding. It is found that the peak at 594 cm^{-1} appears after the deposition of Pd. In addition, the broad peak located at about 3500 cm^{-1} splits into two peaks at about 3200 and 3600 cm^{-1} . The difference of the two spectra implies that a new product should be formed due to the displacement reaction of TiN. The peak at 594 cm^{-1} corresponds to the IR-active vibration of TiF_6^{2-} .¹⁵ In addition, the splitting of the broad peaks should demonstrate the formation of $(\text{NH}_4)_2\text{TiF}_6$. This apparent discrepancy still existed when TiN powder was used instead of TiN film.

We attempt to deduce the result obtained so far. Initially the Pd^{2+} forms a $\text{PdCl}_x\text{F}_y^{2-}$ complex with square planar structure after F^- is added to the solution. Then, F^- serves as a bridging ligand to transfer electrons released from the substrate. Meanwhile, F^- also breaks the Ti-N bonding by virtue of their strong affinity for electrons. At the final stage, titanium is oxidized to form TiF_6^{2-} . However, it is difficult to directly examine the product from N^{3-} . Theoretically, there are two possible routes for N^{3-} participating in a displacement reaction. The first is that N^{3-} may be oxidized together with Ti^{3+} to form N_2 , *i.e.*, N^{3-} also releases electrons. Or N^{3-} may retain its oxidation state and solvate into water to form an ammonium ion. We therefore propose the following two mechanisms.¹⁶

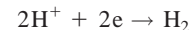
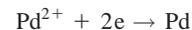
Mechanism 3a, oxidation of TiN, N^{3-} is oxidized



Mechanism 3b, oxidation of TiN, N^{3-} solvates to form NH_3



Reduction of Pd^{2+} and H^+



The above two mechanisms include the generation of gas, corresponding to what had been observed during the displacement reaction. Apparently, the ratio between the consumption of Pd^{2+} and the generation of TiF_6^{2-} in the two mechanisms does not correlate with each other. Therefore, ICP-AES was employed to estimate the ratio between the two species, as shown in Table II. Samples A and B were of identical composition except for the presence of TiN powder in sample B. Sample C provided further information for the dissolution of TiN powder into BHF solution, which contained an identical amount of TiN powder. According to the relative concentration of each component, the ratio between the consumption of Pd^{2+} and the generation of titanium ions can be computed as follows

$$\frac{\text{Pd}}{\text{Ti}} = \frac{375.74 - 7.02/106.4}{678 - 5.28/47.88} = 4.02$$

The above computation indicates that each Pd atom deposited on the surface generates four titanium ions oxidized from TiN film. The ICP-AES result is also convincing evidence for Ti^{4+} when combined with that of IR spectra. If the condition follows mechanism

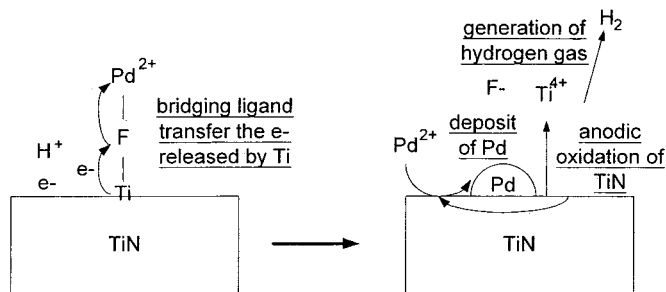


Figure 21. Displacement deposition of Pd: oxidation of TiN and evolution of hydrogen gas.

3a, there will be too many electrons released from TiN, and the ratio between consumed Pd^{2+} and generated Ti^{4+} would be 0.5, which does not correspond to that of the ICP-AES result. It is known that the electrons released from the oxidized Ti are enough to provide the reduction of Pd^{2+} . Hence, the formation of nitrogen gas, *i.e.*, the oxidation of N^{3-} , should not occur in this reaction. The most favorable product species thus becomes NH_3 (NH_4^+ in aqueous solution) by the nature of N atoms. Both the formation of NH_4^+ , which could result in neutralization, and the evolution of hydrogen gas, will eliminate H^+ . Thus, the increase in pH by the reaction was capable of illustrating the formation of NH_3 , and the experimental result corresponded to the description, irrespective of the concentration of F^- . In conclusion, the observed gas during the reaction is hydrogen and the ICP-AES result implies that mechanism 3b is more plausible. Moreover, Ti^{3+} is presumably oxidized to TiF_6^{2-} of which the oxidation state increases to four, which possess the most stable electronic structure among all oxidation states of Ti. The scheme of mechanism 3b is described in Fig. 21.

In order to evaluate the feasibility of using this displacement reaction in an industrial process, the electrodeposition of copper was then executed on the nitride/Si substrate which had been pretreated by Pd displacement deposition. In Fig. 22a, different sizes of copper crystal can be observed. Theoretically, the Pd deposit is capable of serving as a platform for subsequent Cu electroplating, because of its lower electrical resistance ($10.54 \mu\Omega \text{ cm}$) in comparison with the barrier nitride (about $100\text{--}200 \mu\Omega \text{ cm}$). In addition, Cu^{2+} could be driven by an electric current selectively being adsorbed onto the Pd atoms. Nevertheless, owing to the poor uniformity of Pd deposition, copper grew into two different types following the nucleation and growth processes. Cu crystals with a larger grain size (about $5\text{--}10 \mu\text{m}$) may be formed with the aid of Pd seeds. On the other hand, smaller grains grew directly on top of the barrier and experienced greater resistance through crystal growth. Thus, the temperature for Pd deposition was raised to about 50°C . The reaction rate of Pd displacement increased accordingly, and the uniformity of Pd seeding was improved. The morphology of Cu deposits under the improved conditions is shown in Fig. 22b. The problem of pinholes was also mitigated and more uniform Cu deposits were obtained.

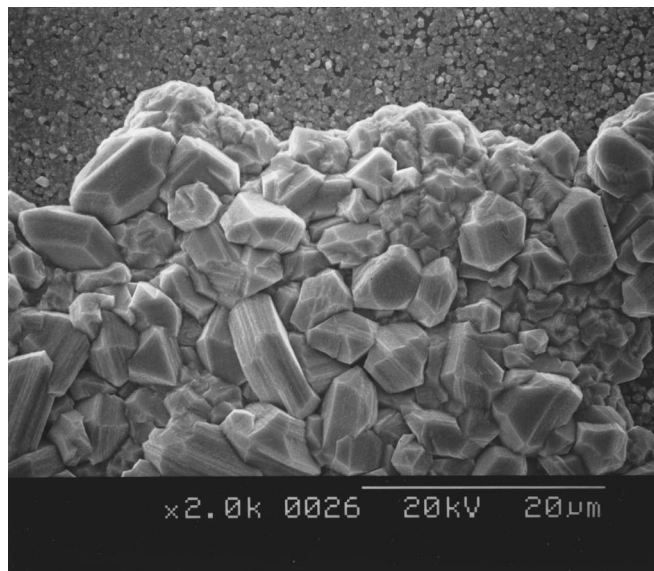
Conclusions

A displacement reaction occurs between nitride barriers and Cu^{2+} , Ag^+ , and Pd^{2+} in the presence of F^- , resulting in spontaneous metal deposition. Moreover, similar metal reduction occurs on the Si substrate solely when F^- exists. From the results of AES, XPS, SEM, NMR, ICP-AES, Raman and IR spectroscopy, we believe that a displacement reaction of TiN takes place according to the following mechanism

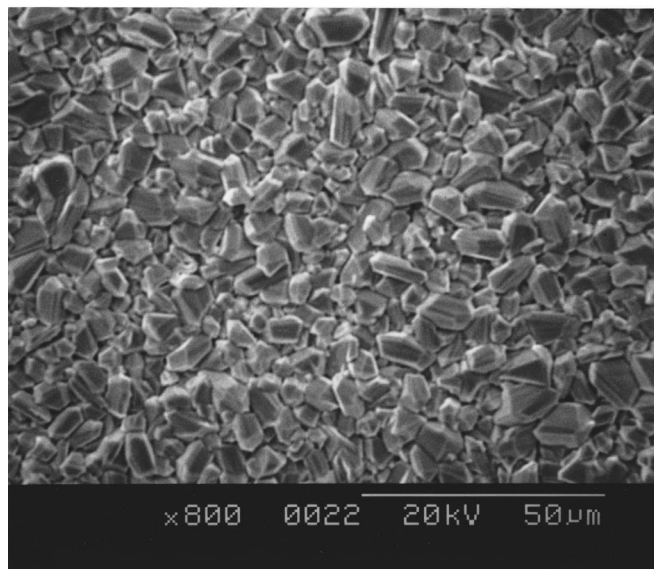
Oxidation of TiN, N^{3-} solvates to form NH_3



Reduction of Pd^{2+} and H^+

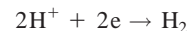
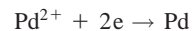


(a)



(b)

Figure 22. (a) Different size of Cu deposit on nitride surface pretreated by Pd displacement. (b) Cu deposit after Pd displacement at 40°C .



Initially Pd^{2+} forms a square planar $\text{PdCl}_x\text{F}_y^{2-}$ complex after F^- is added to the solution. Then, F^- serves as bridging ligand and breaks the Ti-N bonding by virtue of its strong electron affinity. At the final stage, titanium is oxidized to form TiF_6^{2-} . Meanwhile, N^{3-} is solvated to form NH_4^+ , while Pd^{2+} receives electrons and deposits. Moreover, under proper conditions, including an elevated bath temperature, Pd can serve as a platform for subsequent Cu electrodeposition via this method.

In addition, a slight precipitation of $(\text{NH}_4)_2\text{SiF}_6$, occurs because F^- corrodes the exposed SiO_2 . The underlying Si then releases electrons which are captured by metal ions.

National Hsing-Hua University assisted in meeting the publication costs of this article.

References

1. P. C. Andricacos, *Electrochem. Soc. Interface*, **8**(1), 32 (1999).
2. P. C. Andricacos, C. Uzoh, J. O. Dukovic, J. Horkans, and H. Deligianni, *IBM J. Res. Dev.*, **42**, 567 (1998).
3. J. Torres, J. L. Mermet, R. Madar, G. Crean, T. Gessner, A. Bertz, W. Hasse, M. Plotner, F. Binder, and D. Save, *Microelectron. Eng.*, **34**, 119 (1996).
4. R. D. Mikkola, Q. T. Jiang, and B. Carpenter, *Plat. Surf. Finish.*, **87**, 81 (2000).
5. T. Nitta, T. Ohmi, T. Hoshi, S. Sakai, K. Sakaibara, S. Imai, and T. Shibata, *J. Electrochem. Soc.*, **140**, 1131 (1993).
6. G. S. Sandhu, S. G. Meikle, and T. T. Doan, *Appl. Phys. Lett.*, **62**, 240 (1993).
7. M. H. Staia, E. S. Puchi, D. B. Lewis, J. Cawley, and D. Morel, *Surf. Coat. Technol.*, **86-87**, 432 (1996).
8. M. H. Tsai, S. C. Sun, C. P. Lee, H. T. Chiu, and S. C. Wu, *Thin Solid Films*, **270**, 531 (1995).
9. K. N. Cho, C. H. Han, K. B. Noh, and J. G. Lee, *Jpn. J. Appl. Phys., Part 1*, **37**, 6502 (1998).
10. V. M. Dubin and Y. Shacham-Diamand, *J. Electrochem. Soc.*, **144**, 898 (1997).
11. H. P. Fung and C. C. Wan, in *Electrochemical Processing in ULSI Fabrication and Semiconductor/Metal Deposition II*, P. C. Andricacos, P. C. Searson, C. Reidsema-Simpson, P. Allongue, J. L. Stickney, and G. M. Oleszek, Editors, PV 99-9, p. 194, The Electrochemical Society Proceedings Series, Pennington, NJ (1999).
12. J. O'Kelly, K. Mongey, Y. Gobil, J. Torres, P. Kelly, and G. Crean, *Microelectron. Eng.*, **50**, 473 (2000).
13. J. Moulder, W. Stickle, P. Sobol, and K. Bourben, *Handbook of X-Ray Photoelectron Spectroscopy*, p. 220, Perkin-Elmer Corp., Eden Prairie, MN (1992).
14. T. C. Franklin, *Plat. Surf. Finish.*, **30**, 415 (1987).
15. K. Nakamoto, *Infrared and Raman Spectra of Inorganic and Coordination Compounds*, p. 189, John Wiley & Sons, New York (1997).
16. Y. Wu, Y. Y. Wang, and C. C. Wan, in *Electrochemical Processing in ULSI Fabrication and Electrodeposition Of and On Semiconductors IV*, J. L. Stickney, K. Kondo, P. C. Andricacos, and P. C. Searson, Editors, PV 2001-8, The Electrochemical Society Proceedings Series, Pennington, NJ, In press.